

‘Negative’ intensity patches in angular variations of CMB as a probe of the period of reionization

A. Doroshkevich^{1,2}, & V. Dubrovich^{1,3}

¹Theoretical Astrophysics Center, Juliane Maries Vej 30, DK-2100 Copenhagen Ø, Denmark

²Keldysh Institute of Applied Mathematics, Russian Academy of Sciences, 125047 Moscow, Russia

³SAO, 196140, Pulkovo, St.-Petersburg, Russia,

Accepted ..., Received ; in original form

ABSTRACT

The observational tests for the period of reionization of the universe are discussed. We show that this period can be observed as *negative* intensity patches of the CMB radiation with the amplitude $\delta T/T \sim 10^{-5}$ and the angular sizes $\theta_T \sim 10$ angular seconds in range of the wavelength $0.1 \text{ cm} \leq \lambda \leq 1 \text{ cm}$. The expected number density and frequency dependence of the amplitude permit to recognize this effect and to discriminate it from the noise. This method applied to the small scale variations of CMB temperature complements well the traditional spectral approach.

The number density and the amplitude of observed ‘negative’ intensity patches depend upon the redshift of reionization that allow to estimate roughly this redshift. The ionized bubbles formed just before the period of reionization could also be seen as the highest peaks. The expected results are sensitive to the Jeans scale at the period of reionization, to the small scale shape of the primordial power spectrum and to the mass of dark matter particles.

Key words: cosmology: cosmic microwave background — — theory – galaxies: formation.

1 INTRODUCTION

The analysis of the cosmic microwave background radiation (CMB) anisotropy generated after reionization of the universe has been began in Sunyaev & Zel’dovich (1980) (static and kinematic Sunyaev-Zel’dovich effect), Kaiser (1984) and Ostriker & Vishniac (1986). Later on various aspects of this problem were discussed in many publications (see, e.g., Tegmark, Silk, Blanchard, 1994; Hu, Scott & Silk 1994; Persi 1995; Tegmark & Silk 1995; Aghanim et al. 1996; Hu & White (1996); Knox, Scoccimarro & Dodelson 1998; Gruzinov & Hu 1998; Peebles & Juszkievicz 1998, Griffiths, Barbosa & Liddle 1999; Haiman & Knox 1999; Peterson et al. 1999; Weller, Battye & Albrecht 1999; Rees 1999; Molnar & Birkinshaw 2000; Cooray, Hu, & Tegmark 2000; Benson et al. 2001). Various possible sources of such perturbations were considered – from linear and second order perturbations and up to CMB scattering within a set of high density clouds and clusters of galaxies.

Firstly the expected variations of the CMB temperature have been calculated in Vishniac (1987) where has been noted that, for larger l , the power spectrum of the temperature variations reproduces well the spectrum of perturbations and is defined by the reionization epoch. Recent publications repeat the same calculations, concentrate more

attention on the impact of nonlinearity and inhomogeneity of reionization (Peebles & Juszkievicz 1998; Gruzinov & Hu 1998; Knox, Scoccimarro & Dodelson 1998; Jaffe & Kamionkowski 1998; Haiman & Knox 1999; Hu 2000), and use numerical simulations of the reionization (Springel et al. 2000; Bruscoli, Ferrara & Ciardi 2000; Gnedin and Jaffe 2000) for direct calculations of the power spectrum of CMB variations, C_l . It is interesting that results based on simulations differ in some respects from theoretical expectations. Thus, for example, Peebles & Juszkievicz (1998) demonstrate the small impact of moderate nonlinearity which can be expected during the period of reionization. The toy model discussed in Gruzinov & Hu (1998) shown that the ionization in patches also cannot essentially distort expectations obtained under assumption of homogeneous reionization. In simulations, however, the noticeable impact of both effects was found. The more detailed discussions and comparisons of these results with theoretical expectations are needed to clarify the validity of theoretical assumptions and representativity of simulations.

Here we turn back to the simplest case of linear theory and consider the small scale angular variations of the CMB temperature produced by velocity perturbations after the reionization of the universe (linear Doppler and Ostriker-

arXiv:astro-ph/0108213v1 13 Aug 2001

Vishniac effects). Recent discussions of this problem in publications cited above use the popular spectral description of expected small scale variations of $\delta T/T$. This spectrum cannot be, however, found with both MAP and Planck missions and to do this special extensive observations are required. Here we demonstrate that the more simple direct analysis of the map of CMB temperature variations provides also valuable information about the reionization epoch and in some respect could be more perspective.

As was shown in Kaiser (1984) and Ostriker & Vishniac (1986), $\delta T/T$ generated after epoch $z = z_\tau$ where the universe last is optically thick, $\tau_e(z_\tau) \sim 1$, are small because the different phases of any single plane wave cancel each other out, and the main effect is generated at the epoch of reionization at $z = z_{ri}$ and/or at redshifts when $\tau_e(z_\tau) \sim 1$. For earlier reionization when $z_{ri} \geq z_\tau$ and the universe is optically thick, $\tau_e(z_{ri}) \gg 1$, the $\delta T/T$ averages the peculiar motion across the Hubble length $c/H(z_\tau)$ at the epoch of last scattering (Sunyaev 1978). In the case, the damping of perturbations is defined by the variation of optical depth, $\tau_e(z)$, with redshift. For later reionization, $z_{ri} \leq z_\tau$, the dynamic of reionization becomes important and random angular variations of z_{ri} can also be seen.

The damping depends upon the velocity coherent length, l_v , defined by the initial power spectrum. Some characteristics of density and velocity fields in the models with Harrison-Zel'dovich initial power spectrum and Bardeen et al. (1986) transfer function were found in Demiański & Doroshkevich (1999; 2001). Here we show that for such models this damping is moderate and an amplitude $\delta T/T \sim 10^{-5} - 3 \cdot 10^{-6}$ can be expected in minute and subminute ranges.

2 PERIOD OF REIONIZATION

The processes of reheating and reionization of intergalactic gas have been widely discussed during last years (see, e.g., Gnedin & Ostriker 1997; Baltz, Gnedin & Silk 1997; Haiman, Rees & Loeb 1997; Tegmark et al. 1997; Abel et al. 1998; Silk & Rees 1998; Haehnelt, Natarajan, & Rees 1998; Miralda-Escudé et al. 2000; Haiman, Abel & Rees 1999; Haiman & Loeb 1999; Shapiro, Iliev & Raga 1999; more references in Haiman & Knox 1999) but up to now it is far from clarity.

It is agreed that the reionization is produced by the first population of relatively low massive galaxies with

$$M \geq M_{min} \sim 10^7 M_\odot \frac{\Omega_b}{0.1} \frac{0.5}{h} \left[\frac{10}{1+z_{vir}} \right]^{3/2}, \quad (2.1)$$

(Haiman, Rees & Loeb 1997) where z_{vir} is redshift of formation of virialized cloud. The formation of more massive galaxies, quasars and black holes is also discussed as at redshifts $z \sim 3 - 5$ both bright galaxies and quasars are observed (see, e.g., Steidel et al. 1998; Fan et al. 2000).

The hard problem is a reasonable estimate of luminosity of objects responsible for reionization and of the efficiency factor of reionization, E , that is a ratio of ionized and collapsed volumes. Available now estimates of this factor vary from $E = 114$ and up to $E = 10^2 [20/(1+z)]^3$ (Haiman & Loeb 1999; more references in Knox, Scoccimarro & Dodelson 1998, and Haiman & Knox 1999). Evidently, this factor

directly relates to the fraction of matter, $f_m(z_{ri})$, accumulated by objects with $M \geq M_{min}$ at the redshift of reionization, $z \sim z_{ri}$, and the mass conservation shows that

$$f_m(z_{ri}) \approx 1/E(z_{ri}) \quad (2.2)$$

Our estimates based on the statistics of high density clouds formation (Demiański & Doroshkevich 2001) confirm that for both values of E cited above and for larger mass of the heaviest DM particles $M_{DM} \geq 1$ GeV the reionization is quite possible at redshifts $z_{ri} \sim 40 - 20$ when objects with $M \geq M_{min}$ incorporate $\sim 2 - 8\%$ of the matter. At the same redshifts amorphous irregular clouds with a moderate overdensity above the mean density accumulate $\sim 15 - 40\%$ of matter. Some part of these clouds can be unstable. The latest fraction increases up to $\sim 80\%$ at redshifts $z \sim 4 - 5$ that is consistent with results obtained with high resolution simulations (see, e.g., Zhang et al. 1998). The expected fraction of homogeneously distributed gas at the period of reionization is

$$f_g(z_{ri}) \sim 0.4 - 0.7, \quad (2.3)$$

for $z_{ri} \sim 20 - 40$, respectively.

These numerical estimates are obtained for the CDM-like primordial power spectrum discussed in Sec. 3. They are very sensitive to the shape of small scale primordial power spectrum and mass of DM particles. More conservative approach to the problem of reionization can be found in Benson et al. (2001) where $z_{ri} \sim 10$ is discussed. Observations of small scale $\delta T/T$ will significantly clarify this problem.

The reionization and reheating take place at the period when only a small fraction of baryonic matter is accumulated by high density clouds. As was shown in Peebles & Juskiewicz (1998), these clouds do not distort the expected variations of CMB temperature. Non the less, the reheating of baryonic component suppresses the small scale baryonic perturbation in scales lesser then the Jeans scale, R_J ,

$$R_J \approx \frac{a_s(1+z_{ri})}{H(z_{ri})} \approx \frac{0.12\sqrt{T_4}}{\sqrt{\Omega_m z_{ri}}} h^{-1} \text{Mpc}, \quad (2.4)$$

where a_s , $T_4 = T/10^4 K \sim 1$ and Ω_m are the sound speed, the expected temperature of reionized gas and the mean density of the universe. It essentially restricts the expected variations of the CMB temperature in small scale and, in fact, leads to the cutoff in the power spectrum of the CMB variations at $l \sim 3 \cdot 10^4 - 10^5$ (Sec. 6).

3 BASIC COSMOLOGICAL MODEL AND CHARACTERISTICS OF THE DENSITY AND VELOCITY FIELDS

3.1 Parameters of cosmological model

As a basic model, we use the spatially flat Λ CDM model (Jenkins et al. 1998) with parameters

$$\Omega_m = 0.3, \quad \Omega_b = 0.03, \quad h = 0.7, \quad \sigma_v(0) = 650 \text{ km/s}, \quad (3.1)$$

where Ω_m & Ω_b are dimensionless density of dark matter (DM) and baryonic components, $\Omega_\Lambda = 1 - \Omega_m$, $h = H_0/100 \text{ km/s/Mpc}$ is dimensionless Hubble constant, and $\sigma_v(0)$ is a velocity dispersion at redshift $z = 0$. The analysis of this simulation (Jenkins et al. 1998; Demiański et al.

2001) shown that it reproduces well characteristics of large scale matter distribution observed at small redshifts and, so, can be used as a basic model for further investigations.

Here we are interested in larger redshifts, $z \geq 10$, where the influence of Ω_Λ becomes negligible and the main relations are simplified. For such redshifts we have

$$H(z) \approx H_0 \sqrt{\Omega_m} (1+z)^{3/2}, \quad (3.2)$$

$$\frac{\sigma_v(z)}{\sqrt{3}c} = \frac{1.6 \cdot 10^{-3}}{\sqrt{z}} \sqrt{\frac{0.3}{\Omega_m}} \frac{\sigma_v(0)}{650 \text{ km/s}} = \frac{w_0}{\sqrt{z}}.$$

The velocities of baryonic component suppressed at $z \sim 1000$ are practically restored already at $z \sim 50$.

Distances along a line of sight are measured by the conformal time and linked to the redshifts as follows:

$$\eta(z) \approx \eta_0 [f_\Lambda - (1+z)^{-1/2}], \quad (3.3)$$

$$\eta_0 = \frac{2c}{H_0 \sqrt{\Omega_m}} \approx 1.1 \cdot 10^4 \sqrt{\frac{0.3}{\Omega_m}} h^{-1} \text{ Mpc},$$

$$f_\Lambda \approx \frac{3}{\sqrt{\pi}} \left(\frac{\Omega_m}{\Omega_\Lambda} \right)^{1/6} = 1.47 \left(\frac{\Omega_m}{0.3} \frac{0.7}{\Omega_\Lambda} \right)^{1/6}$$

3.2 Characteristics of density and velocity fields

To estimate the efficiency of the formation $\delta T/T$ we use two characteristics of peculiar velocity field, namely, the coherence length, l_v , and the correlation functions of velocities. For the Harrison-Zel’dovich initial power spectrum of perturbations, $p(k) \propto k$, and for the Bardeen et al. (1986) transfer function, $T^2(x)$, the velocity coherent length was introduced in Demiański & Doroshkevich (1999) as follows:

$$l_v^{-2} = \int_0^\infty k T^2(k/k_0) dk = m_{-2} k_0^2, \quad k_0 = \frac{\Gamma h}{1 \text{ Mpc}},$$

$$\Gamma = \Omega_m h \sqrt{\frac{1.68 \rho_\gamma}{\rho_{rel}}}, \quad m_{-2} = \int_0^\infty x T^2(x) dx \approx 0.023,$$

$$l_v \approx \frac{6.6}{\Gamma} \sqrt{\frac{0.023}{m_{-2}}} h^{-1} \text{ Mpc} = 33 h^{-1} \text{ Mpc} \left(\frac{0.2}{\Gamma} \right), \quad (3.4)$$

where ρ_γ & ρ_{rel} are the density of CMB and relativistic particles (photons, neutrinos etc.).

3.2.1 Doppler effect

The normalized velocity correlation function can be approximated by an expression (Demiański & Doroshkevich 1999):

$$\frac{\langle v_i(\mathbf{r}_1) v_j(\mathbf{r}_2) \rangle}{\sigma_v^2(0)} = F_1(x) \delta_{ij} + x_i x_j F_2(x), \quad (3.5)$$

$$\mathbf{x} = \frac{\mathbf{r}_1 - \mathbf{r}_2}{l_v}, \quad x = |\mathbf{x}|, \quad \sigma_s^2 = \frac{1}{2\pi^2} \int_0^\infty dk p(k),$$

$$F_1(x) = \frac{3}{2\pi^2 \sigma_s^2} \int_0^\infty dk p(k) \frac{j_1(kl_v x)}{kl_v x} \approx \frac{1}{1+x+ax^2},$$

$$F_2(x) = \frac{dF_1}{dx} = -\frac{3}{2\pi^2 \sigma_s^2} \int_0^\infty dk k^2 p(k) \frac{j_2(kl_v x)}{(kl_v x)^2}$$

where \mathbf{r}_1 and \mathbf{r}_2 are unperturbed coordinates of points at $z = 0$ and the parameter $a \approx 0.3$ can be expressed through other moments of the power spectrum.

Fits of the perturbation amplitude to the CMB anisotropy (Bunn & White 1997) link model parameters (3.1) with COBE data and we get:

$$\sigma_s \approx 13.4 h^{-1} \text{ Mpc} \left(\frac{h}{0.7} \right) \left(\frac{\Omega_m}{0.3} \right)^{0.2} \left(\frac{T_Q}{15 \mu\text{K}} \right),$$

$$w_0 \approx 0.65 \frac{H_0 \sigma_s}{c \sqrt{3}}.$$

where T_Q is the amplitude of quadrupole component of anisotropy. For the projection of the correlation function (3.4) on two directions, $\bar{\gamma}_1$ and $\bar{\gamma}_2$, we get:

$$F(x, \mu) = \mu \xi_v(x) - (1-\mu^2) \frac{|\mathbf{r}_1| |\mathbf{r}_2|}{l_v^2} F_2(x), \quad (3.6)$$

$$\bar{\gamma}_1 \bar{\gamma}_2 = \mu \approx 1 - \theta^2/2, \quad 1 - \mu \ll 1.$$

Here the function

$$\xi_v(x) = F_1(x) + x^2 F_2(x) \approx \frac{1 - ax^2}{(1+x+ax^2)^2}, \quad (3.7)$$

describe the velocity correlation along a line of sight (for $\mu = 1$).

To estimates of the variations of CMB temperature at the period of reionization we will use the point separation measured along a line of sight (3.3) and for the characteristic correlation angle we have

$$\theta_v = \frac{l_v}{\eta_0 f_\Lambda} \approx 7' \frac{0.7}{h} \sqrt{\frac{0.3}{\Omega_m}} \frac{1.47}{f_\Lambda}. \quad (3.8)$$

3.2.2 Ostriker-Vishniac effect

The cross correlation of velocity and density fields is described by the second order power spectrum of perturbation as this correlation vanishes for the first order perturbations. This correlation leads to second order correction for the Doppler perturbations and to the Ostriker - Vishniac effect. The second order spectrum of baryonic component is found in Appendix A.

The normalized correlation functions, G_1 and G_2 , and the amplitude of CMB temperature variations for the OV-effect, σ_b , can be written as follows:

$$G_{ij}(y) = \langle v_i(\mathbf{r}_1) \delta(\mathbf{r}_1) v_j(\mathbf{r}_2) \delta(\mathbf{r}_2) \rangle / \sigma_b^2 = \quad (3.9)$$

$$[2G_1(y) + y^2 G_2(y)] \delta_{ij} - y_i y_j G_2(y),$$

$$\mathbf{y} = \frac{\mathbf{r}_1 - \mathbf{r}_2}{r_J}, \quad \alpha_J = k_0 R_J \approx 10^{-2} \frac{h}{0.7} \sqrt{T_4 \frac{\Omega_m}{0.3} \frac{20}{z_{ri}}},$$

$$r_J \approx 0.75 R_J \ln \left(\frac{1}{\alpha_J} \right) \approx 0.17 \sqrt{T_4 \frac{0.3}{\Omega_m} \frac{20}{z_{ri}}} h^{-1} \text{ Mpc},$$

$$G_1(y) \approx \frac{1}{(1+y^2)^{0.6}}, \quad G_2(y) \approx -\frac{1.2}{(1+y^2)^{1.6}},$$

$$\sigma_b^2 = f_{OV}^2 \sigma_v^2(0), \quad f_{OV} \approx \ln \left(\frac{1}{\alpha_J} \right) \left(\frac{h}{0.7} \right)^2 \left(\frac{\Omega_m}{0.3} \right)^{1.2} \frac{T_Q}{15 \mu\text{K}}.$$

Here as before \mathbf{r}_1 and \mathbf{r}_2 are unperturbed coordinates of points at $z = 0$ and σ_b is an amplitude of perturbations. The Jeans scale, R_J , were introduced by (2.4).

For the projection of the correlation function (3.9) on two directions, $\vec{\gamma}_1$ and $\vec{\gamma}_2$, we get:

$$\gamma_i \gamma_j G_{ij} = 2\mu G_1(x) + (1 - \mu^2) \frac{|\mathbf{r}_1||\mathbf{r}_2|}{r_0^2} G_2(x), \quad (3.10)$$

$$\vec{\gamma}_1 \vec{\gamma}_2 = \mu \approx 1 - \theta^2/2, \quad 1 - \mu \ll 1,$$

and for the characteristic correlation angle we have

$$\theta_J = \frac{r_J}{\eta_0 f_\Lambda} \approx 2'' \sqrt{T_4 \frac{20}{z_{ri}} \frac{1.47}{f_\Lambda}}. \quad (3.11)$$

4 VARIATIONS OF OPTICAL DEPTH

Now it is generally agreed that the reionization starts with formation of separate bubbles number and size of which increase with time. At redshifts $z = z_{ri}$ these bubbles merge together and the high ionization degree, $f_i(z_{ri}) \sim 1$, is achieved. The maximal optical depth of the universe achieved due to reionization can be written as follows:

$$\tau_{max} = c\sigma_c \int_0^\infty \frac{n_e(x)dx}{xH(x)} = \tau_0 z_{ri}^{3/2} K_f, \quad (4.1)$$

$$\tau_0 = 1.4 \cdot 10^{-3} \sqrt{\frac{0.3}{\Omega_m} \frac{h\Omega_b}{0.02}},$$

$$K_f = \frac{3}{2} \int_0^\infty \left(\frac{x}{z_{ri}}\right)^{3/2} f_i(x) \frac{dx}{x} \geq 1.$$

Here c & $\sigma_c = 6.6 \cdot 10^{-25} \text{cm}^2$ are the speed of light and the Thompson cross section, the density of electrons $n_e(z) \approx 1.2 \cdot 10^{-5} \Omega_b (1+z)^3 \text{cm}^{-3}$, and a factor K_f takes proper account of dynamic of reionization. Thus, $K_f = 1$ for the instantaneous reionization at $z = z_{ri}$ and $K_f \geq 1$ when partial ionization is reached at larger redshifts and $z^{3/2} f_i(z)$ slow decreases for $z \geq z_{ri}$. In particular, this function integrates separate ionized bubbles formed before the full reionization and, so, is a random function of line-of-sight.

Three models of $\delta T/T$ generation should be considered. For earlier reionization when $\tau_{max} \gg 1$ we have

$$z_\tau = z_0 = \tau_0^{-2/3} = 80 \left(\frac{\Omega_m}{0.3}\right)^{1/3} \left(\frac{0.02}{\Omega_b h}\right)^{2/3}. \quad (4.2)$$

In the case, the characteristics of $\delta T/T$ depend only upon parameters of the basic cosmological model. For later reionization, when $\tau_{max} \geq 1$ but $z_{ri} \leq z_0$ we have

$$z_0 \geq z_\tau = z_{ri} K_f^{2/3} \geq z_{ri}. \quad (4.3)$$

For $\tau_{max} \leq 1$, the generation of $\delta T/T$ is driven by the dynamic of the process of reionization and final estimates of $\delta T/T$ become more uncertain. In particular, in the case random angular variations of τ_{max} can be observed.

When the CMB radiation is scattered in a cloud with a proper size $\sim l_v$ and a correlated velocity along a line-of-sight $v(z)$, the temperature perturbations of CMB observed with angular resolution smaller than a cloud size, $\theta_{cl} \sim 10'$, are

$$\left(\frac{\delta T}{T}\right) = \sigma_c n_e(z) l_v v(z)/c \approx \quad (4.4)$$

$$2.3 \cdot 10^{-6} \frac{l_v}{33h^{-1}\text{Mpc}} \left(\frac{1+z}{20}\right)^{3/2} \frac{\Omega_b h^2}{0.015} \frac{\sigma_v(0)}{650\text{km/s}}.$$

This amplitude is comparable with estimates of Gruzinov & Hu (1998) and with the expected small scale variations of the CMB temperature (Secs. 5.1, 5.2). The measurable amplitude of $\delta T/T \sim 10^{-5}$ can be achieved only within ionized bubbles with an extremal velocity $\sigma_v \sim 3\sigma_v(0)$. Formation of such bubbles is not forbidden even at larger redshifts but it becomes more probable in a course of merging of many low massive bubbles just before the reionization. For later reionization, $\tau_{max} \leq 1$, such bubbles could be observed as a random angular variation of z_{ri} and τ_{max} .

Factors $f_i(z)$ and K_f characterize the redshift variation of number density of the homogeneously distributed ionized gas and must be corrected for probable matter concentration within low massive clouds. Small fraction of denser clouds provides the reionization but essential fraction of gas can be accumulated within irregular clouds with various sizes and moderate overdensity above the mean density, $\delta\rho/\rho \sim 5 - 10$. As was shown by Peebles & Juskiewicz (1998), action of this effect cannot substantially change the expected optical depth, τ , and parameters z_0 and z_τ but for generality we will include it in our consideration.

Now the possible formation of such clouds with variety of morphology is widely discussed. For example, in simulations at redshift $z \sim 4$ (see, e.g., Zhang et al. 1998) up to 90 - 95% of gas are found to be accumulated within such amorphous clouds that explains the suppression of observed Gunn-Peterson effect. Efficiency of such concentration at larger redshifts depends upon the amplitude and coherent length of density field and, so, is sensitive to the mass of DM particles and the shape of initial power spectrum.

Here we will characterize action of this effect by the mean fraction of homogeneously distributed gas at redshift of reionization, $f_g = \langle f_g(z) \rangle \leq 1$. The expected values of f_g can vary in wide range, $0.05 \leq f_g \leq 1$ with redshift, coherent length l_ρ and dynamic of reionization. This factor can be incorporated in relations (3.1) - (3.4) by the substitution of $f_g \Omega_b$ in place of Ω_b that increases our previous estimates of z_0 and decreases estimates of τ_{max} . The redshift variations of $f_g(z)$ can be incorporated in the factor K_f by the substitution of $f_g(z) f_i(z) / \langle f_g(z) \rangle$ in place of $f_i(z)$.

5 VARIATIONS OF CMB TEMPERATURE

The perturbations of CMB temperature caused by Doppler effect are defined as follows:

$$\left(\frac{\delta T}{T}\right)_D = \int_0^\infty \frac{v(z)}{c} e^{-\tau_e(z)} d\tau_e(z). \quad (5.1)$$

(see, e.g., Hu, Scott & Silk 1994; Peebles & Juskiewicz 1998). Here $v(z)$ is a line-of-sight peculiar velocity and, as before, $\tau_e(z)$ is the optical depth due to Thompson scattering of CMB. For a cloud situated at redshift z with a proper size

$$D_{cl} = cH^{-1}(z)\Delta z, \quad \Delta z = H(z)D_{cl}/c \ll 1, \quad (5.2)$$

this expression becomes identical to (4.4). In general case it defines a random function $\delta T/T$. For Gaussian initial perturbations the probability distribution function of $\delta T/T$ is

also Gaussian and its properties are characterized by the variance, σ_D^2 :

$$\sigma_D^2 = \int_0^\infty d\tau_e(z_1) d\tau_e(z_2) \frac{\langle v(z_1)v(z_2) \rangle}{c^2} e^{-\tau_e(z_1)-\tau_e(z_2)} \quad (5.3)$$

$$= \int_0^\infty d\tau_e(z_1) d\tau_e(z_2) \frac{\sigma_v(z_1)\sigma_v(z_2)}{3c^2} \xi_v(z_1, z_2) e^{-\tau_e(z_1)-\tau_e(z_2)}.$$

Here the function $\xi_v(z_1, z_2)$ describes the correlation of peculiar velocities along a line-of-sight and, therefore, the expected damping of perturbations at the period of reionization and at smaller redshifts. This expression can also be obtained directly from Eqs. (25)–(32) of Hu, Scott & Silk (1994).

5.1 Amplitude of CMB fluctuations generated by the Doppler effect

For the basic model, the correlation of velocities along a line-of-sight are described by (3.5) with $\mu = 1$ and

$$x = \frac{1}{\kappa_D} \left| \sqrt{\frac{z_{ri}}{z_1}} - \sqrt{\frac{z_{ri}}{z_2}} \right|,$$

$$\kappa_D \approx \frac{l_v \sqrt{z_{ri}}}{\eta_0} \approx 1.35 \cdot 10^{-2} \sqrt{\frac{z_{ri}}{20} \frac{0.3}{\Omega_m} \frac{0.7}{h}}. \quad (5.4)$$

For $\kappa_D \ll 1$ the expression (5.3) can be rewritten more explicitly as follows:

$$\sigma_D^2 \approx \frac{9}{4} \tau_0^{2/3} w_0^2 \int_0^\infty dx_1 dx_2 \xi(z_\tau x_1, z_\tau x_2) \exp[-\tau_0(x_1^{3/2} + x_2^{3/2})]$$

$$= 2.25 \tau_0^{2/3} w_0^2 \kappa_D K_D, \quad \tau_{max} \gg 1, \quad (5.5a)$$

$$\sigma_D^2 \approx \frac{9}{4} \tau_0^2 w_0^2 z_{ri}^2 \int_0^1 dx_1 dx_2 \xi(z_{ri} x_1, z_{ri} x_2) e^{-\tau(z_1)-\tau(z_2)}$$

$$= 2.25 \tau_0^2 w_0^2 z_{ri}^2 \kappa_D K_D, \quad \tau_{max} \leq 1. \quad (5.5b)$$

Here κ_D describes the main damping of perturbations while the factor $K_D \leq 1$ takes proper account of damping and weights it along a line-of-sight. K_D weakly depends upon small redshifts, slowly decreases with κ_D and $K_D \approx 0.25 - 0.5$ for the range of interest, $\kappa_D \sim 0.01 - 0.1$. For $\kappa_D \leq 0.01$ K_D decreases $\propto \kappa_D \ln(1/\kappa_D)$. Parameters w_0 , and τ_0 were introduced by (3.2) and (4.1).

For the hypothetical case of earlier reionization, $\tau_{max} \gg 1$, $z_\tau = z_0$, we have

$$\sigma_D \approx 3 \cdot 10^{-5} \left(\frac{f_g \Omega_b}{0.03} \right)^{1/6} \left(\frac{0.15}{\Omega_m h^2} \right)^{5/6} \frac{\sigma_v(0)}{650 \text{ km/s}}, \quad (5.9)$$

This result confirms that for so earlier reionization, $z_{ri} \geq z_\tau \sim 80 (f_g \Omega_b h / 0.02)^{-2/3} (\Omega_m / 0.3)^{1/3}$, $\tau_{max} \gg 1$ the measurable variations of $\delta T/T \sim 10^{-5}$ can be expected with a high probability even if the velocities of baryonic component are not yet restored and $\sigma_v(0) \leq 650 \text{ km/s}$. In the case, the amplitude depends mainly upon basic parameters of cosmological model and random angular variations of z_{ri} caused by the random spatial distribution of earlier ionized bubbles are not seen.

For more realistic case of later reionization we have

$$\sigma_D \approx 2 \cdot 10^{-3} w_0 \frac{f_g \Omega_b}{0.03} \left(\frac{z_{ri}}{20} \frac{0.3}{\Omega_m} \frac{0.7}{h} \right)^{3/4} K_f^{5/6}, \quad (5.10)$$

where K_f is given by (4.1), and $f_g \leq 1$ is the mean fraction of homogeneously distributed gas at $z = z_{ri}$. The random factor K_f characterizes the dynamic of reionization along a line-of-sight.

The measurable variations of $\delta T/T \sim 10^{-5}$ can be expected with a reasonable probability for $f_g \Omega_b z_{ri} K_f \geq 0.5$ when at least higher peaks in Gaussian field can be really observed. The largest clouds ionized at higher redshifts magnify K_f and can be seen as random higher amplitude patches.

5.2 Amplitude of CMB fluctuations generated by the Ostriker-Vishniac effect

Amplitude of the CMB fluctuations generated by the Ostriker-Vishniac effect can be found in the same manner:

$$\sigma_{OV}^2 = \sigma_D^2 \frac{\kappa_J K_J f_{OV}^2}{\kappa_D K_D z_{ri}^2}, \quad (5.11)$$

$$\kappa_J K_J = 2 \int_0^{z_{ri}} \frac{dz_1 dz_2 G_1(z_1, z_2)}{(1+z_1)(1+z_2)} e^{-\tau(z_1)-\tau(z_2)}$$

$$\kappa_J = \frac{r_J \sqrt{z_{ri}}}{\eta_0} = 0.7 \cdot 10^{-4} \sqrt{T_4 \frac{z_{ri}}{20}}, \quad K_J \approx 53.$$

$$\sigma_{OV} \approx 0.2 \sigma_D \left(\frac{h}{0.7} \frac{\Omega_m}{0.3} \right)^{1.5} \left(\frac{20}{z_{ri}} \right) T_4^{1/4} \frac{w_0}{1.7 \cdot 10^{-3}}$$

Here the function $G_1(z_1, z_2)$ describes the correlation of perturbations along a line-of-sight, parameters $\eta_0, r_J, f_{OV}, \kappa_D, K_D$ & σ_D were introduced in (3.3), (3.9), (5.4), (5.5) and (5.10).

6 ANGULAR CORRELATION FUNCTION AND POWER SPECTRUM OF CMB VARIATIONS

6.1 Power spectra

The power spectra of CMB variations can be found directly from the power spectra of perturbations (Vishniac 1987, Appendix B & C):

$$\frac{l^2 C_l}{2\pi} \approx 6.4 \cdot 10^{-12} \frac{l}{\alpha} T^2 \left(\frac{l}{\alpha} \right), \quad (6.1)$$

$$\frac{l^2 C_l}{2\pi} \approx 10^{-12} \left(\frac{l}{\alpha} \right)^3 T_b \left(\frac{l}{\alpha} \right). \quad (6.2)$$

for Doppler and Ostriker-Vishniac effects, respectively. In both cases the power spectra of CMB variations reproduce well the transfer functions of perturbations, namely T^2 & T_b . The transfer function of baryonic perturbations, T_b , is introduced in (A.8). As was shown in Appendix B & C for larger l , $C_l \propto z_{ri}$ for the Doppler and $C_l \propto \sqrt{z_{ri}}$ for the Ostriker-Vishniac effects, that verifies the domination of period of reionization for both effects (Vishniac 1987).

These power spectra are plotted in Fig. 1 together with

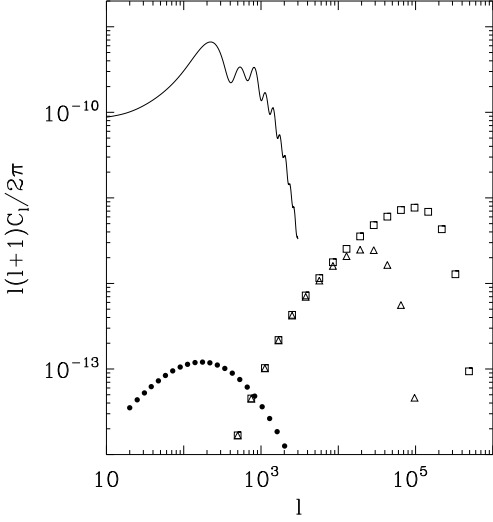


Figure 1. The spectrum of the CMB temperature anisotropy generated by the Doppler (dots) and OV-effects for $\alpha_J = 0.05$ (triangles) & 0.01 (squares) as compared with the expected primary CMB anisotropy (solid line).

the spectrum of the expected primary CMB anisotropy. The variations of the amplitude with cosmological parameters and redshifts of reionization are described by (5.10), (5.11), (B.4) and (C.3).

6.2 Correlation functions

The angular correlation function of the CMB fluctuations generated by both effects, $w(\theta)$, can be found from the general expressions (3.6) and (3.9) using functions ξ_v, F_2, G_1 & G_2 and the point separation

$$x^2 \approx \kappa_D^{-2} \left(\sqrt{\frac{z_{ri}}{z_1}} - \sqrt{\frac{z_{ri}}{z_2}} \right)^2 + \left(\frac{\theta}{\theta_v} \right)^2 \left[1 - \frac{f_\Lambda^{-1}}{\sqrt{1+z_1}} - \frac{f_\Lambda^{-1}}{\sqrt{1+z_2}} \right]^2, \quad (6.3)$$

for the Doppler effect and similar relation for Ostriker - Vishniac effect.

The normalized correlation functions are plotted in Figs. 2 & 3 for $z_{ri} = 20$ and 40 . For $40 \geq z_{ri} \geq 10$ these functions can be well fitted by expressions

$$w(x) \approx (1 + x^2)^{-\gamma}, \quad x = \theta/\theta_0, \quad (6.4)$$

$$\gamma_D \approx 0.43, \quad \theta_0 \approx 4.2\theta_v \approx 30',$$

$$\gamma_J \approx 0.15, \quad \theta_0 \approx 4\theta_J \approx 8'',$$

for Doppler and Ostriker-Vishniac effects, respectively.

6.3 Characteristics of peaks

The small expected amplitude of the CMB variations (5.10) and (5.11) indicates that the observational determination of the power spectrum C_l is hard problem and at the first step only high peaks with $\delta T/T \sim 2 - 3 \sigma_{OV} \sim 10^{-5}$ could be

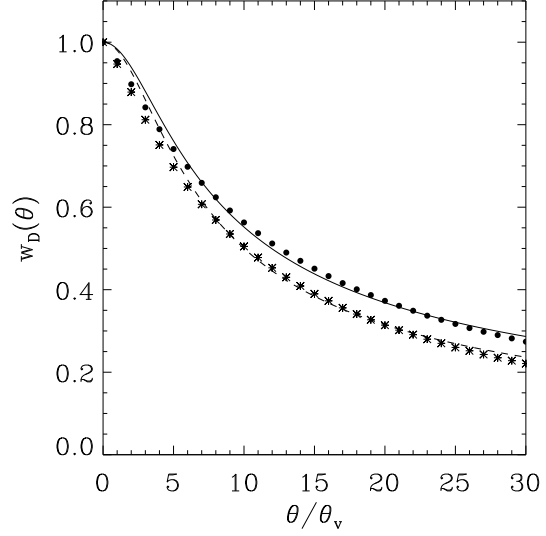


Figure 2. Correlation functions of CMB fluctuations generated by the Doppler effect for $z_{ri} = 20$ (points) and $z_{ri} = 40$ (stars) together with fits (6.4).

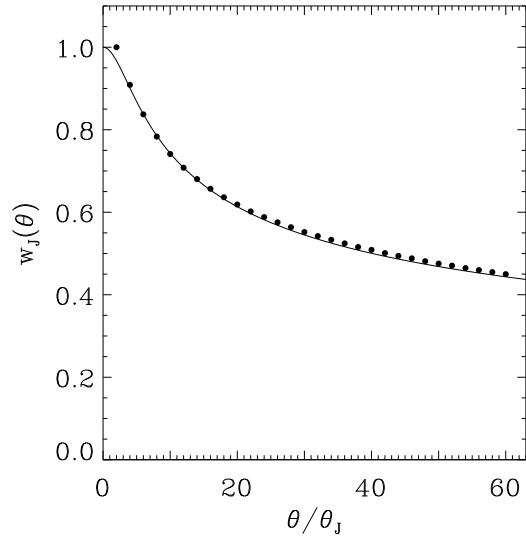


Figure 3. Correlation functions of CMB fluctuations generated by the Ostriker-Vishniac effect for $z_{ri} = 20$ together with fits (6.4).

actually observed. This means that the peak distribution is also an important characteristic which helps to discriminate the cosmological patches from the noise.

The expected shape of peaks is described by the correlation function (6.4) whereas their number density is given by the Minkowski Functional. Application of this approach to the variations of CMB temperature have been discussed in Winitzki & Kosowsky (1997), Schmalzing & Gorski (1997), Novikov, Feldman & Shandarin (1998), Dolgov et al. (1999). For the Gaussian distribution of the temperature variations with the correlation function (6.4) we get for the number density of positive peaks higher than threshold amplitude, $\nu = \delta T/T/\sigma_T$,

$$\langle n_{max}(> \nu) \rangle = \frac{1 + \gamma}{2\pi\sqrt{3}\theta_0^2} f(\nu), \quad (6.5)$$

where the function $f(\nu)$ characterizes a threshold dependence of n_{max} . This dependence helps to select and identify the peaks under consideration for larger statistics of the peaks with different ν (Novikov et al. 2001).

The expected number density of higher Doppler peaks is:

$$\langle n_{max}(> \nu = 1) \rangle \approx (113')^{-2}, \quad (6.6a)$$

$$\langle n_{max}(> \nu = 2) \rangle \approx (250')^{-2}. \quad (6.6b)$$

The expected distribution function of CMB fluctuations generated by the *nonlinear* OV – effect is also close (but not identical) to the Gaussian one. Indeed, as is well known, the distribution function for the product of two normal variates is

$$f(\nu) = 1/\pi K_0(|\nu|) \propto \exp(-|\nu|), \quad |\nu| \gg 1$$

where K_0 is the modified Bessel function (Stuart & Ord 1994). However, the integration of perturbations along a line-of-sight makes again the distribution of CMB fluctuations similar to the Gaussian one. The expected deviations from the Gaussianity are small for $|\nu| \leq 1$ but hold more strong for larger $|\nu|$. The degree of these deviations depends upon the actual number of ”clouds” within the integral (5.1) along a line-of-sight and, therefore, upon the redshift of reionization. It increases for later reionization when small amplitude of the CMB variations is also expected.

The application of Minkowski functional to some non-Gaussian statistics of CMB had been illustrated in many publications (see, e.g., Coles & Barrow 1987, Coles 1988). Their results verify that, for example, deviations between the Gaussian and χ_n^2 statistics with $n \geq 30$ do not exceed 10 – 12%. The significant difference between characteristic angles as given by (3.11) and (6.4) ($\theta_0 \sim 4\theta_j$) as well as a large difference between σ_{OV} (5.11) and the possible contribution of a separate cloud with a size $\sim r_J$ indicate that the number of ”clouds” along a line of sight is $\gg 20$ and the expected degree of the deviations from the Gaussianity can be moderate even for the highest peaks.

Because of this we will apply expressions (6.5) for the first estimates of surface density of higher OV-peaks as well. We have:

$$\langle n_{max}(> \nu = 1) \rangle \approx (37'')^{-2}, \quad (6.7a)$$

$$\langle n_{max}(> \nu = 2) \rangle \approx (82'')^{-2}. \quad (6.7b)$$

$$\langle n_{max}(> \nu = 3) \rangle \approx (5')^{-2}. \quad (6.7c)$$

The same expressions describe the mean number density of the negative peaks, $n_{min}(< \nu = -1)$, $n_{min}(< \nu = -2)$ and $n_{min}(< \nu = -3)$. These estimates show that with the angular resolution $\sim 8 - 10''$ peaks with the amplitude $\delta T/T \sim 10^{-5}$ can be observed with a reasonable probability.

6.4 Negative intensity patches

The discrimination of the cosmological $\delta T/T$ becomes more easy if we concentrate more attention on the investigation of *negative* intensity patches (Dubrovich 2000, Springel, White & Hernquist 2000). The expected Gaussian distribution of cosmological $\delta T/T$ predicts equally probable patches with

both positive and negative intensity, but the negative intensity patches cannot be produced by any background or foreground sources excluding only Sunyaev-Zel’dovich (SZ) effect in clusters of galaxies some of which can be identified with their x-ray radiation (at least at $z \leq 1$, Refregier et al. 2000).

To discriminate the noise, SZ and Doppler patches their different frequency dependence can be used (Sunyaev & Zel’dovich 1980). The Doppler shift discussed above does not change the spectrum of CMB and the frequency variations of intensity of Doppler and OV patches are

$$\delta F_D(\chi) = F_0 \frac{\chi^4 e^{-\chi}}{(1 - e^{-\chi})^2} \frac{\delta T}{T}, \quad \chi = h\nu/kT_\gamma, \quad (6.8)$$

$$F_0 = 2.7 \cdot 10^{-15} \text{ ergs}(\text{cm}^2 \text{ s sr Hz})^{-1}, \quad T_\gamma = 2.73\text{K}$$

where χ is dimensionless frequency of radiation. The maximal intensity of these patches, $\delta F/F_0 \approx 4.9(\delta T/T)$, is achieved at $\chi \approx 3.8$. It drops up to $\delta F/F_0 \approx \delta T/T$ at $\chi \sim 1$ and $\chi \sim 8.6$.

The frequency dependence of SZ effect (Zel’dovich & Sunyaev 1969; Weller, Battye & Albrecht 1999) is

$$\delta F_{sz}(\chi) = F_0 y_c \frac{\chi^4 e^{-\chi}}{(1 - e^{-\chi})^2} \left[\chi \frac{1 + e^{-\chi}}{1 - e^{-\chi}} - 4 \right], \quad (6.9)$$

where y_c is the dimensionless Compton parameter. This intensity is negative at $\chi \leq 3.8$ and positive at $\chi \geq 3.8$, maximal $\delta F_{sz}/F_0 = 6.8y_c$ and minimal $\delta F_{sz}/F_0 = -4.1y_c$ are achieved at $\chi = 6.5$ and $\chi = 2.3$, respectively.

If observations are performed with a set of wavelengths in range $1 \text{ cm} \geq \lambda \geq 0.1 \text{ cm}$ then the different frequency dependence of (6.8) and (6.9) allows to discriminate between patches produced by Sunyaev-Zel’dovich and Doppler and OV effects.

The free-free emission of reionized plasma can, in principle, restrict the existence of negative intensity patches. It depends upon many factors such as the temperature, ionization degree and small scale clustering of plasma at high redshifts estimates of which are strongly model dependent. However, the available estimates of the observed intensity of the free-free emission

$$F_{ff} \leq 3 \cdot 10^{-19} \text{ ergs}(\text{cm}^2 \text{ s sr Hz})^{-1} = 10^{-4} F_0 \quad (6.8)$$

(Bartlett & Stebbins 1991) confirm that within discussed range of wavelengths the cosmological patches can be observed. More detailed discussion of the background and foreground can be found in White et al. (1999), Cooray, Hu & Tegmark (2000), and Refregier, Spergel & Herbig (2000).

7 SUMMARY AND DISCUSSION

Different methods of investigation of the ”dark age” in the history of the universe evolution between $z = 1000$ and $z = 5$ were discussed during last years (see references in Sec. 1) but most attention has been concentrated on the traditional spectral approach to the investigation of small scale variations of CMB temperature that requires extensive observations with high precision. The expected amplitudes of cosmological $\delta T/T$ obtained in Sec. 6 show that the more simple direct observation of higher positive and especially negative

intensity patches can successfully complement the spectral investigations.

The patches can be observed with already available techniques using the aperture synthesis and/or interferometry (White et al. 1999; Dubrovich & Partridge 2000). Radio-frequency interferometry offers the advantage of virtually complete freedom from atmospheric emission and other systematic effects. Now such telescopes as the ACTA (Australia) and VLA (USA) in cm as well as IRAM (Plateau de Bure) and JCMT (Hawaii) by SCUBA in mm and submm ranges can be used to search for the patches.

To discriminate reliably between Doppler, OV and SZ patches, wavelength $\lambda \leq 2$ mm should be used. In future most promising will be ALMA, to be completed in the next decade. It will operate in all the atmospheric windows from 1 cm to 0.45 mm and will be able to detect sources at $\lambda \leq 0.1$ cm with the angular resolution and sensitivity of the present VLA at cm wavelengths.

Higher amplitudes (5.9), $\sigma_T \sim 3 \cdot 10^{-5}$, expected for the hypothetical case of very early reionization, $z_{ri} \geq z_0 \sim 80$, depend mainly upon cosmological parameters, $\Omega_m h^2$ and $\sigma_v(0)$. Perhaps, so early reionization is possible for the tilted power spectra with an excess of power in small scales. In the case, distortions of the first generation of $\delta T/T$ can be essential even at angular scale $\sim 1^\circ$ (Griffiths, Barbosa & Liddle 1999; Tegmark & Zaldarriaga 2000).

More realistic scenario of later reionization, $z_{ri} \sim 40 - 20$, predicts the existence of patches with $\sigma_T \sim 0.5 \cdot 10^{-5}$ as given by (5.10), (5.11) which can be observed at least as a system of the separate highest peaks. The amplitude is larger for earlier period of reionization due to growth of both z_{ri} and $f_g(z_{ri})$. Reionization at $z_{ri} \geq 20$ is possible for the tilted power spectra with an excess of power in small scales and/or for the Harrison- Zel'dovich power spectrum with extremely heavy DM particles, $M_{DM} \sim 10^{18} - 10^{21}$ keV. Existence of such particles is now discussed as a possible interpretation of observed high energy cosmic rays (Bertou, Boratav, & Letessier-Selvon 2000; Nagano & Watson 2000). In the case, possible random angular variations of z_{ri} caused by random merging of earlier ionized bubbles can also be observed as the separate highest peaks.

The angular distribution of the patches is driven by the spatial correlation of the peculiar velocity field. The same field is also responsible for a large scale distribution of galaxies and their strong concentration within filaments and walls (see, e.g. Demiański & Doroshkevich 1999, Demiański et al. 2000). This concentration is observed in deep surveys such as the Las Campanas Redshift Survey (Shectman et al. 1996) and Durham/UKST redshift Survey (Ratcliffe et al. 1996) and is well reproduced in numerous simulations. For example, the mean separation of richer observed walls, $D_{sep} \sim 50 - 60 h^{-1}$ Mpc, is about twice of the velocity coherent length, l_v , as defined by (3.4). This implies that the correlated distribution of negative patches and, perhaps, the appearance of the *network of patches* with few angular minutes sizes can also be expected. The correlation of higher peaks was discussed in Heavens & Sheth (1999).

Similar network of negative patches with the angular sizes $\theta \sim 1 - 2'$ and angular separation $\theta_{sep} \sim 5'$ was firstly observed by Carlstrom, Joy & Grego (1996) with 30 GHz receiver of Owens Valley Radio Observatory in a course of investigations of Sunyaev-Zel'dovich effect toward two clusters

of galaxies. The statistical reliability of these small amplitude negative patches is not enough, and these observations should be repeated with better sensitivity and in wider range of wavelengths, $1 \text{ cm} \geq \lambda \geq 0.1 \text{ cm}$. The frequency dependence of the amplitude and statistical properties discussed in Sec. 6 allows to test the attribution of the patches as cosmological and generated at redshifts $z \geq 10$.

Acknowledgments

This paper was supported in part by Denmark's Grundforskningsfond through its support for an establishment of Theoretical Astrophysics Center. It was prepared during VKD visit TAC, and he is grateful TAC for hospitality. We are grateful to P. Naselsky for stimulating conversations. We also wishes to acknowledge support from the Center for Cosmo-Particle Physics "Cosmion" in the framework of the project "Cosmoparticle Physics".

REFERENCES

- Abel T., Anninos P., Norman M.L., & Zhang Yu., 1998, ApJ., 508, 518
Aghanim N., Désert F.X., Puget J.L., & Gispert R., 1996, A&A, 311, 1
Baltz E.A., Gnedin N.Y., Silk J., 1997, ApJ., 493, L1.
Bardeen J.M., Bond J.R., Kaiser N., Szalay A., 1986, ApJ., 304, 15
Bartlett J.G., & Stebbins A., 1991, ApJ., 371, 8
Benson A.J., Nusser A., Sugiyama N., Lacey C.G., 2001, MNRAS, 320, 153
Bertou X., Boratav M., Letessier-Selvon A., 2000, IJMP, A15, 2181
Bruscoli M., Ferrara A., Fabbri R., Ciardi B., 2000, MNRAS, 318, 1068
Bunn E.F. & White M., 1997, ApJ., 480, 6
Carlstrom J.E., Joy M., Grego L., 1996, ApJ., 456, L75
Coles P., Barrow J.D., 1987, MNRAS, 228, 407
Coles P., 1988, MNRAS, 234, 309
Cooray A., Hu W., Tegmark M., 2000, ApJ., 540, 1
Demiański M. & Doroshkevich A., 1999, MNRAS, 306, 779
Demiański M. & Doroshkevich A., 2001, MNRAS, submit.
Demiański M. et al. 2001, MNRAS, submitted
Dolgov A. et al. 1999, IJMP D., 8, 189
Dubrovich V.K., 2000, Ast.L., submitted
Dubrovich V.K., Partridge R.B., 2000, A&AT, v.20, in press
Fan X. et al., 2000, AJ., 120, 1167
Gnedin N.Y., & Ostriker J.P., 1997, ApJ., 486, 581
Gnedin N.Y., & Jaffe A.H., 2000, ApJ., in press, astro-ph/0008469
Gradshteyn I.S. & Ryzhik I.M., 1994, Table of Integrals, Series, and Products, Academic Press, Inc., Boston, New York, London.
Griffiths L.M., Barbosa D., & Liddle A.R., 1999, MNRAS, 308, 854
Gruzinov A., & Hu W., 1998, ApJ., 508, 435
Haiman Z., Rees M., & Loeb A., 1997, ApJ., 476, 458
Haiman Z., & Knox L., 1999, "Microwave Foregrounds", eds. A. De Oliveira-Costa & M. Tegmark (ASP, San Francisco, 1999), p. 227
Haiman Z., & Loeb A., 1999, ApJ., 519, 479
Haiman Z., Abel T., & Rees M., 2000, ApJ., 534, 11
Haehnelt M.G., Natarajan P., Rees M.J., 1998, MNRAS, 300, 817
Heavens A.F. & Sheth R.K., 1999, MNRAS, 310, 1062
Hu W., Scott D., Silk J., 1994, Phys.Rev.D, 49, 648
Hu W., 2000, ApJ, 529, 12

Hu W., White M., 1996, A&A, 315, 33
 Jaffe A.H., & Kamionkowski M., 1998, Phys.Rev. D, 58, 043001
 Jenkins A. et al., 1998, ApJ., 499, 20.
 Kaiser N., 1984, ApJ., 282, 374
 Knox L., Scoccimarro R., & Dodelson S., 1998, PhysRev., 81, L2004
 Miralda-Escudé J., Haehnelt M., Rees M., 2000, ApJ., 530, 1
 Molnar S.M., Birkinshaw M., 2000, ApJ., 537, 542
 Nagano M., & Watson A.A., 2000, Rew.Mod.Phys., 72, 689
 Novikov D., Feldman H.A. & Shandarin S.F., 1999, IJMP, D8, 291
 Novikov D. et al., 2000, IJMP, in press
 Ostriker J.P., & Vishniac E.T., 1986, ApJ., 306, L51
 Peebles P.J.E., & Juszkiewicz R., 1998, ApJ., 509, 483
 Persi F.M., 1995, ApJ., 441,1
 Peterson J.B. et al., 1999, astro-ph/9907276
 Ratcliffe, A., Shanks, T., Broadbent, A., et al., 1996, MNRAS, 281, L47
 Rees M.J., 1999, 9th Annual October Astrophysics Conference in Maryland. Eds. S. Holt & E. Smith. American Institute of Physics Press, 1999, p. 13
 Refregier A., Komatsu E., Spergel D.N., Pen U.L., 2000, Phys.Rev.D, in press, astro-ph/9912180
 Shapiro P.R., Iliiev I.T., & Raga A.C., 1999, MNRAS, 307, 203
 Shectman S.A., et al., 1996, ApJ, 470, 172
 Schmalzing J. & Gorski K.M., 1998, MNRAS, 297, 355
 Silk J., & Rees M.J., 1998, A&A, 331, L1
 Springel V., White M., & Hernquist L., 2001, ApJ., in press, astro-ph/0008133
 Steidel C.C., Adlerberger K.L., Dickinson M., Giavalisco M., Pettini M., & Kellogg M., 1998, ApJ., 492, 428.
 Stuart A., & Ord J.K., 1994, Kendall’s Advanced Theory of Statistics, vol.1, Distribution Theory, Edward Arnold, London, Melburn, Auckland.
 Sunyaev R.A., 1978, in Large Scale Structure of the Universe, ed. M.S. Longair & J. Einasto (Dordrecht: Reidel), 393
 Sunyaev R.A., Zel’dovich Ya.B., 1980, MNRAS, 190, 413
 Tegmark M., Silk J., Blanchard A., 1994, ApJ., 420, 484.
 Tegmark M., & Silk J., 1995, ApJ., 441, 458
 Tegmark M., Silk J., Rees M., Blanchard A., Abel T., Palla F., 1997, ApJ., 474, 1.
 Tegmark M., & Zaldarriaga M., 2000, ApJ., 544, 30
 Vishniac E.T., 1987, ApJ., 322, 597
 Weller J., Battye R.A., Albrecht A., 1999, Phys.Rev.D, 60, 103
 White M., Carlstrom J.E., Dragovan M., Holzzapfel W.L., 1999, ApJ., 514, 12
 Winitzki S. & Kosowsky A., 1998, MNRAS, 297, 355
 Zel’dovich Ya.B., Sunyaev R.A., 1969, Ap&SS, 4, 301
 Zhang Yu., Meiksin A., Anninos P., Norman M.L., 1998, ApJ., 495, 63

Appendix A

Second order power spectrum for the Ostriker-Vishniac effect

The cross correlation of velocity and density fields is described by the second order power spectrum of perturbations. This correlation vanishes for the first order perturbations. This correlation leads to second order correction for the Doppler perturbations and to the Vishniac - Ostriker effect.

The second order spectrum can be written as follows:

$$\langle v_i(\mathbf{r}_1)\delta(\mathbf{r}_1)v_j(\mathbf{r}_2)\delta(\mathbf{r}_2) \rangle = \int d^3k \Phi_{ij}(k) \exp[i\mathbf{k}(\mathbf{r}_1 - \mathbf{r}_2)],$$

where v_i and δ are peculiar velocities and relative density perturbations. Here

$$\Phi_{ij}(k) = \int d^3q \langle v_i(k)\delta(k)v_j(q)\delta(q) \rangle = \quad (A.1)$$

$$\left(\delta_{ij} - \frac{k_i k_j}{k^2} \right) \Phi_1(k) + \frac{k_i k_j}{k^2} \Phi_2(k),$$

$$\Phi_1(k) = \frac{1}{2} \int d^3q \frac{p(q)}{q^2} \frac{p(|\mathbf{k} - \mathbf{q}|)}{(\mathbf{k} - \mathbf{q})^2} \frac{k^2 q^2 - (\mathbf{kq})^2}{k^2 q^2} [k^2 - 2(\mathbf{kq})]$$

$$\Phi_2(k) = \int \frac{d^3q}{q^2} p(q) p(|\mathbf{k} - \mathbf{q}|) \frac{\mathbf{kq}}{k^2} \left(\frac{k^2 - (\mathbf{kq})}{(\mathbf{k} - \mathbf{q})^2} + \frac{(\mathbf{kq})}{q^2} \right)$$

The function Φ_1 describes the Vishniac - Ostriker effect while the function Φ_2 gives the second order contribution to the Doppler effect. Both functions characterize the DM perturbations and at $k \rightarrow 0$ $\Phi_1 \propto \Phi_2 \propto k^2$ while for $k \rightarrow \infty$, $\Phi_1 \propto \Phi_2 \propto k^{-3}$ and they are sensitive to the small scale nonlinear damping of perturbations. These functions are well fitted by expressions:

$$\Phi_1(x) \propto x^2(1 + 2.5x + 4x^2 + 0.37x^{2.5})^{-2}, \quad (A.2)$$

$$\Phi_2(x) \propto x^2(1 + 1.45x + 5.37x^2 + 1.25x^{2.5})^{-2}. \quad (A.3)$$

where $x = k/k_0$. The function $k^2\Phi_1(k/k_0)$ plays a role of the power spectra for OV-effect.

To describe perturbations of baryonic component and to take into account the pressure of reionized gas we will substitute in equations (A.1) instead of $p(k)$

$$p(k)j_0^2(kR_J), \quad R_J = \frac{a_s(1+z)}{H(z)} \approx \frac{0.12\sqrt{T_4}}{\sqrt{\Omega_m z_{ri}}} h^{-1} \text{Mpc}. \quad (A.4)$$

Here a_s and $T_4 = T/10^4 K \sim 1$ are the sound speed and the expected temperature of reionized gas. This factor suppresses the small scale perturbation and instead of (A.2) we get for perturbations of baryonic component

$$\Phi_b(x) \approx \Phi_1(x) \exp(-0.6\alpha_J^2 x^2), \quad (A.5)$$

$$x = k/k_0, \quad \alpha_J = k_0 R_J = 10^{-2} \frac{h}{0.7} \sqrt{T_4 \frac{\Omega_m}{0.3} \frac{20}{z_{ri}}}.$$

With this spectrum we get for the normalized spatial correlation functions, G_1 and G_2 , the transfer function T_b and the amplitude of OV-effect, σ_b :

$$G_{ij}(y) = \langle v_i(\mathbf{r}_1)\delta(\mathbf{r}_1)v_j(\mathbf{r}_2)\delta(\mathbf{r}_2) \rangle / \sigma_b^2 = \quad (A.6)$$

$$[2G_1(y) + y^2 G_2(y)] \delta_{ij} - y_i y_j G_2(y), \quad y = \frac{r_{12}}{r_J} = \frac{|\mathbf{r}_1 - \mathbf{r}_2|}{r_J},$$

$$r_J \approx 0.75 R_J \ln \left(\frac{1}{\alpha_J} \right) \approx 0.17 \sqrt{T_4 \frac{0.3}{\Omega_m} \frac{20}{z_{ri}}} h^{-1} \text{Mpc}$$

$$G_1(y) = \frac{3}{m_b} \int_0^\infty dx x^2 T_b(x) \frac{j_1(kr_{12})}{kr_{12}} \approx \frac{1}{(1+y^2)^{0.6}}$$

$$G_2(y) = -\frac{3}{m_b} \int_0^\infty dx x^4 T_b(x) \frac{j_2(kr_{12})}{(kr_{12})^2} \approx -\frac{1.2}{(1+y^2)^{1.6}}$$

$$T_b(x) \approx \frac{x^2 \exp(-0.6\alpha_J^2 x^2)}{(1 + 2.5x + 4x^2 + 0.37x^{2.5})^2}, \quad x = k/k_0, \quad (A.7)$$

$$m_b = \int_0^\infty dx x^2 T_b \approx 0.116 \ln^2(\alpha_J), \quad (A.8)$$

$$\sigma_b^2 = \int_0^\infty d^3 k \Phi_b(k) = f_{OV}^2 \sigma_s^2, \quad (A.9)$$

$$f_{OV} = \frac{3.7 \cdot 10^{-2} \sigma_s^2 \sqrt{m_b}}{l_b^2 m_{-2}^{3/2}} \approx \ln\left(\frac{1}{\alpha_J}\right) \left(\frac{h}{0.7}\right)^2 \left(\frac{\Omega_m}{0.3}\right)^{1.2} \frac{T_Q}{15\mu K}.$$

Here as before \mathbf{r}_1 and \mathbf{r}_2 are unperturbed coordinates of points at $z = 0$ and σ_b is an amplitude of perturbations.

Appendix B

Power spectrum of CMB generated by Doppler effect after reionization.

To obtain the power spectrum of CMB perturbations generated by the Doppler effect we use the general expression for the angular correlation function

$$C(\mu) = z_{ri}^{-2} \int_0^{z_{ri}} dz_1 dz_2 \left(\mu \xi_v - (1 - \mu^2) \frac{\eta_1 \eta_2}{l_v^2} F_2 \right), \quad (B.1)$$

where $\eta_1 = \eta(z_1)$, $\eta_2 = \eta(z_2)$ and structure functions ξ_v and F_2 are expressed through the power spectrum of primordial perturbations:

$$\begin{aligned} \xi_v &= \frac{3}{m_{-2}} \int_0^\infty x T^2(x) dx [j_0(\eta) - 2j_1(\eta)/\eta] \\ F_2 &= \frac{3}{m_{-2}^2} \int_0^\infty x^3 T^2(x) dx j_2(\eta)/\eta^2, \end{aligned} \quad (B.2)$$

$$\eta = |\vec{\eta}(z_1) - \vec{\eta}(z_2)|, \quad \eta(z) \approx \alpha x \left(f_\Lambda - \frac{1}{\sqrt{1+z}} \right),$$

$$x = k/k_0, \quad \alpha = \frac{2ck_0}{H_0 \sqrt{\Omega_m}} \approx 2 \cdot 10^3 \frac{h}{0.7} \sqrt{\frac{\Omega_m}{0.3}},$$

and $T^2(x)$ is the transfer function of primordial perturbations.

With the 'summation theorem' (Gradshteyn & Ryzhik 1994, 8.533), we get for the power spectrum of CMB perturbations:

$$C_l = \frac{3(l+1/2)}{z_{ri}^2 m_{-2}} \int_0^\infty dx x T^2(x) f_l^2(x), \quad (B.3)$$

$$f_l = \int_0^{z_{ri}} dz e^{-\tau(z)} \frac{dj_l(\eta)}{d\eta}, \quad \eta = \eta(z)$$

This expression is identical to that obtained by Vishniac (1987). It can be applied to any primordial power spectrum and any history of reionization and indicates that C_l depends upon both these factors. We can consider $f_l = \exp[-\tau(z)] dz/d\eta$ as a slowly varying function and rewrite (B.3) as

$$C_l \approx \frac{12z_{ri}l}{m_{-2}\alpha^2} \int_0^\infty \frac{dx}{x} T^2\left(\frac{x}{\alpha}\right) j_l^2(x) \approx \frac{6z_{ri}}{m_{-2}\alpha^2} \frac{1}{l} T^2\left(\frac{l}{\alpha}\right),$$

$$\begin{aligned} \frac{l^2 C_l}{2\pi} &\approx \frac{3}{\pi} \frac{z_{ri}}{\alpha m_{-2}} \frac{l}{\alpha} T^2\left(\frac{l}{\alpha}\right) \\ &\approx 0.5 \frac{l}{\alpha} T^2\left(\frac{l}{\alpha}\right) \frac{z_{ri}}{20} \frac{0.7}{h} \sqrt{\frac{0.3}{\Omega_m}}. \end{aligned} \quad (B.4)$$

Appendix C

Power spectrum of CMB generated by the Ostriker-Vishniac effect after reionization.

To obtain the power spectrum of CMB perturbations generated by the Ostriker-Vishniac effect we use the general expression for the normalized angular correlation function

$$C = \int_0^{z_{ri}} \frac{dz_1}{1+z_1} \frac{dz_2}{1+z_2} \left[\mu G_1 - (1 - \mu^2) \frac{\eta_1 \eta_2}{r_j^2} G_2 \right], \quad (C.1)$$

where $\eta_1 = \eta(z_1)$, $\eta_2 = \eta(z_2)$ and structure functions G_1 and G_2 are expressed through the power spectrum of primordial perturbations (Appendix A) With the 'summation theorem' (Gradshteyn & Ryzhik 1994, 8.533), we get for the power spectrum of CMB perturbations:

$$C_l = \frac{6l^3}{m_b} \int_0^\infty dx x^2 T_b(x) g_l^2(x), \quad (C.2)$$

$$g_l = \int_0^{z_{ri}} \frac{dz}{1+z} e^{-\tau(z)} \frac{j_l(\eta)}{\eta}.$$

This expression is identical to that obtained by Vishniac (1987). The analytical expressions for C_l can be found for $T_b(x) \propto x^0, x^{-2}, x^{-4}, \dots$. They show that the approximate general expression for C_l can be written as follows:

$$\frac{l^2 C_l}{2\pi} \approx \frac{18}{\pi} \frac{\sqrt{z_{ri}}}{m_b} \left(\frac{l}{\alpha}\right)^3 T_b\left(\frac{l}{\alpha}\right) \approx \quad (C.3)$$

$$7 \left(\frac{l}{\alpha}\right)^3 T_b\left(\frac{l}{\alpha}\right) \sqrt{\frac{z_{ri}}{20}} \left(\frac{4.6}{\ln \alpha_J}\right)^2.$$

Numerical factor ~ 1.5 in (C.3) is found by numerical integration of (C.2).